

SINGLE IMAGE LOCAL BLUR IDENTIFICATION

P. Trouvé, F. Champagnat and G. Le Besnerais

J. Idier

ONERA - The French Aerospace Lab
F-91761 Palaiseau, France

LUNAM Université, IRCCyN
(UMR CNRS 6597)
BP 92101, 1 rue de la Noë
44321 Nantes Cedex 3, France

ABSTRACT

We present a new approach for spatially varying blur identification using a single image. Within each local patch in the image, the local blur is selected between a finite set of candidate PSFs by a maximum likelihood approach. We propose to work with a Generalized Likelihood to reduce the number of parameters and we use the Generalized Singular Value Decomposition to limit the computing cost, while making proper image boundary hypotheses. The resulting method is fast and demonstrates good performance on simulated and real examples originating from applications such as motion blur identification and depth from defocus.

Index Terms— Blur identification, motion blur, depth from defocus, spatially varying blur, coded aperture

1. INTRODUCTION

Recorded images are often subject to spatially varying blur coming from defocus, camera or object motions or atmospheric turbulence. It produces an inhomogeneous image quality with local variations due to external characteristics such as scene depth or motion.

Identification of the local PSF (Point Spread Function) offers a way to segment the field of view according to depth or object motion, which are useful clues for many robotic vision purposes. Besides, it allows a local deconvolution step to obtain a motion deblurred image or an image with an extended depth of field.

In this paper, we propose a new method for local blur identification from a single image. The overall image is divided into local patches, on each patch we assume a homogeneous PSF that belongs to a finite set of known candidate PSFs. Candidate PSFs may result from a calibration step [1] or from a parametric model using a finite set of candidate parameters, for instance Gaussian PSF with a set of standard deviations or 1D motion blur with a set of fixed lengths [2].

We have designed a generalized likelihood criterion to select the best PSF candidate on each patch. Our likelihood “integrates out” the input scene patch and thus only depends on PSF and SNR parameters. We propose an efficient and

accurate approach for likelihood evaluation and optimization, using Generalized Singular Value Decomposition (GSVD).

Our method is generic enough to handle any kind of PSF shapes as those resulting from motion blur, defocus blur, or even multi-modal PSF encountered in coded aperture image processing [1]. Efficiency of the proposed approach is demonstrated on synthetic and real data.

1.1. Related work

Single image blur identification can be related to blind deconvolution ([3, 4, 5] and references therein) as both the scene and PSF are unknown. Moreover, dealing with local blurs means that identification has to be done on image patches with a very limited number of data. Such a severely under-determined problem requires additional assumptions on the scene patch and on the PSF.

A popular approach is to model PSF using a reduced set of parameters. Gaussian PSF models are often used to deal with defocus blur [6, 7], while motion blur is often addressed with 1D box functions PSF [2]. Local identification methods dealing with more general PSF shapes are rare, an example is ref. [8] which only assumes a unimodal PSF. Recently, methods able to deal with multimodal PSFs have been proposed in the context of extended depth of field with coded aperture (EDFCA) [1]. Most of these works, except [1, 9], are dedicated to a particular PSF model, while we propose here a generic approach able to handle any kind of PSF shape, or even various PSF shapes in the same image, as encountered in multi-motion scenes.

Dealing with EDFCA, [1] uses a calibrated PSF set and proposes depth estimation based on deconvolution error. This approach yields good results on real images but requires a learning stage to fix some parameters. Besides, the deconvolution assumes a natural prior for the scene, leading to very time consuming large-scale non convex optimizations.

Our approach is more closely related to [2, 9, 10] where the PSF is selected locally thanks to a maximum likelihood criterion (ML). [2] deals with single image motion blur identification, but is limited to image having only one moving object, contrarily to the approach proposed here. In [9], an

EDFCA method is described. It is based on a marginalized likelihood which depends on scene parameters estimated directly from image data. Very good results are obtained on real images but the method seems to be tractable only for a limited number of holes in the coded aperture mask, while our approach has constant cost whatever the PSF shape.

Finally, in contrast to [2, 9, 10] which are dedicated to a particular application, our approach is generic: we demonstrate it on motion blur identification and EDFCA depth estimation. In this context, our main methodological contribution concerns the design of an original likelihood criterion associated to an efficient maximization algorithm.

2. PSF IDENTIFICATION

2.1. Data model

The relation between the scene and the recorded image is usually modeled as a convolution with a PSF. In the case of spatially varying blur, we consider that this model is valid only locally in the image. The local relation between scene and image is usually written in the matrix form:

$$\mathbf{y} = H_k \mathbf{x} + \mathbf{n}, \quad (1)$$

where \mathbf{y} collects the N pixels inside some local patch of the image in the lexicographical representation, \mathbf{x} the M corresponding scene pixels and \mathbf{n} the noise process. H_k is a $N \times M$ convolution matrix within the PSF family $\{H_1, \dots, H_K\}$.

As we consider small patches, care has to be taken concerning boundary hypotheses. In particular the usual periodic model associated to Fourier approaches is not suited here. In the sequel we use "valid" convolutions where the support of x is enlarged with respect to the one of y according to the PSF support so that $M > N$ [11, Section 4.3.2].

2.2. Local criterion

We propose to conduct PSF identification within a ML framework where the unknown scene patch is marginalized out [4, 9]. For simplicity we drop the index of the convolution matrix and use the general notation H .

We assume an isotropic Gaussian prior on the object's gradients so the probability density functions of the object is:

$$p(\mathbf{x}, \sigma_x^2) \propto \exp\left(-\frac{\|D\mathbf{x}\|^2}{2\sigma_x^2}\right).$$

where D is a first order horizontal and vertical derivative operator. Besides, the noise is modeled as a zero-mean white Gaussian noise (WGN) with variance σ_b^2 . For PSF identification we use a marginal likelihood function where the input patch is marginalized out of the problem. The calculation of the integral gives:

$$p(\mathbf{y}|H, \sigma_b^2, \alpha) = (2\pi\sigma_b^2)^{-\frac{N}{2}} \det^+(I - B(\alpha))^{-\frac{1}{2}} e^{-\frac{S(\alpha)}{2\sigma_b^2}} \quad (2)$$

where \det^+ corresponds to the product of the nonzero eigenvalues of $I - B(\alpha)$ and

$$\begin{aligned} S(\alpha) &= \mathbf{y}^T (I - B(\alpha)) \mathbf{y}, \\ B(\alpha) &= H(H^T H + \alpha D^T D)^{-1} H^T. \end{aligned}$$

$\alpha = \sigma_b^2 / \sigma_x^2$ is a regularisation parameter that allows adaptivity according to the Signal to Noise Ratio (SNR). The likelihood depends on H and on two other parameters. To reduce the number of parameters we maximize the likelihood with respect to σ_b^2 in order to deal with a *generalized likelihood* that depends only on H and α [11, Section 3.8.2]. This maximization leads to: $\hat{\sigma}_b^2 = S(\alpha)/N$. Reporting this expression in (2) we obtain that maximizing the likelihood is equivalent to minimize the generalized likelihood function (GL):

$$GL(H, \alpha) = \frac{\mathbf{y}^T (I - B(\alpha)) \mathbf{y}}{\det^+(I - B(\alpha))^{1/(N-n)}}. \quad (3)$$

Where $N - n$ is the number of nonzero eigenvalues of the matrix $I - B(\alpha)$ (here $n = 1$). A more detailed derivation of (3) can be found in [12]. We propose to select the PSF label \hat{k} that corresponds to the joint minimization:

$$(\hat{k}, \hat{\alpha}) = \arg \min_{k, \alpha} GL(H_k, \alpha). \quad (4)$$

2.3. Implementation

Direct calculation of the function (3) is costly because of the dimensions of matrix $H^T H + \alpha D^T D$. The Fourier decomposition is a popular approach for diagonalization of matrices $H^T H$ and $D^T D$ [2]. Fourier approach assumes that the scene is periodic which may be inaccurate for patches whose size is of the same order of the PSF size specially for 2D patches (see section 3). Instead, we propose a decomposition that makes no approximation: the generalized singular value decomposition (GSVD) [12]. For two matrices, H of dimension $N \times P$ and D of dimension $P \times M$, the GSVD writes

$$H = UCX^T \quad D = VSX^T \quad C^T C + S^T S = I \quad (5)$$

where U (respectively V) is a $N \times N$ (resp. $P \times P$) unitary matrix and S and C are diagonal rectangular matrices. With this decomposition we have:

$$B(\alpha) = UC(C^T C + \alpha S^T S)^{-1} C^T U^T, \quad (6)$$

and the GL can be written as:

$$GL(\alpha) = \frac{\sum_{i=1, i \neq j}^N \frac{\alpha s_i^2}{c_i^2 + \alpha s_i^2} z_i^2}{\prod_{i, i \neq j} \left(\frac{\alpha s_i^2}{c_i^2 + \alpha s_i^2} \right)^{1/(N-n)}}. \quad (7)$$

With $\mathbf{c}^2 = \text{diag}(CC^T)$, $\mathbf{s}^2 = \text{diag}(SS^T)$ and $\mathbf{z} = U^T \mathbf{y}$ and j is such as $s_j = 0$. Note that the matrices U, V, C, S and X are independent of α . Thus, it is possible to compute all these

matrices off-line and to store the values of s^2 , c^2 and U . The on-line processing consists in decomposing the whole image in patches, then for each patch the best couple $(\hat{k}, \hat{\alpha})$ is found by exhaustive search over k and a 1D minimization algorithm over α . Once all patches have been processed a map of the local PSF label is obtained. We propose to reject patches that contains no texture using a Canny filter. Indeed, those regions are insensitive to the PSF, so the GL calculation is useless.

3. EXPERIMENTS

3.1. Simulated examples

To simulate the case of 1D PSF identification we built a PSF database composed of horizontal 1D PSF, with a length varying from 1 to 10 pixels. Each line of the output image shown in Fig. 1(a) is obtained by 1D convolution of a line of a natural object (with gray level between 0 and 1) with a PSF whose length is growing from bottom to top. Zero-mean WGN with standard deviation $\sigma = 0.01$ is added to the result. In Fig. 1(b) and (c) are presented the estimated length maps that maximise the proposed GL criterion and the ML criterion of [2] for patch size 1×45 . The GL approach yields significantly better results with a percentage of correct identification of 65% to be compared to 44% for the other approach. In our view, this difference can be explained by the approximate periodic boundary hypothesis implied by Fourier decomposition in [2].

The second simulation test concerns single image EDFCA.

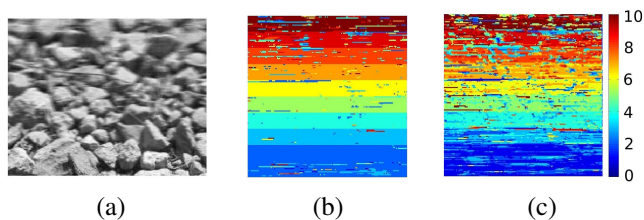


Fig. 1. 1D PSF identification simulation: (a) simulated image. (b) GL with GSVD decomposition. (c) ML algorithm of [2].

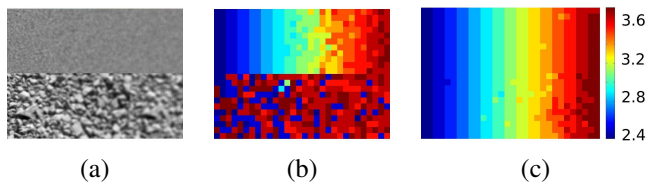


Fig. 2. 2D PSF identification simulation: (a) simulated image. (b) GL with Fourier decomposition, (c) GL with GSVD.

We use the aperture proposed in [1] and the PSFs are obtained with a simulation of the optical system. The focal length is set to 35 mm and the focal plane put at 1.9 m. We consider a set of PSFs that corresponds to depth varying with a step of 0.1 m from 2.4 m to 3.8 m. In Fig. 2 the scene is composed of a white Gaussian noise and a natural image, the gray level

of the whole image varies between 0 and 1. Each vertical segment of the output image shown in Fig. 2(a) is obtained by 2D convolution of a patch of the scene with a PSF of the set, the depth increasing from left to right. Zero-mean WGN with standard deviation $\sigma = 0.01$ is added to the result. The patch size for identification is 21×21 pixels and so are the PSFs size. Fig. 2(b) presents the estimated depth maps using the proposed GL criterion with the Fourier decomposition and Fig. 2(c) the same result with the GSVD. Computation of GL with the GSVD leads to very good identification results. The Fourier transform approach is correct only for high frequency regions of the images, where the periodic model is valid.

Fig. 3(a) shows a collection of natural scenes extracted from the web. Synthetic images are generated by convolution of each of these scenes (with a normalized intensity) with each coded PSF from the previous set and addition of zero-mean WGN of standard deviation 0.01. Fig. 3(b) gives the mean and the standard deviation of estimated depth vs. true ones. Mean values are very close to the true depths and the standard deviation ranges from 10 to 20 cm.

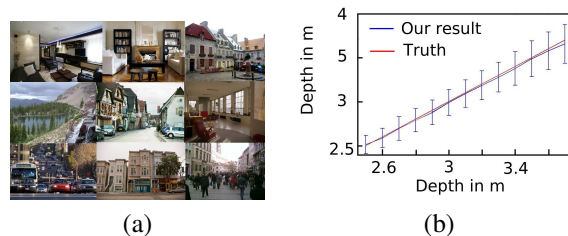


Fig. 3. 2D PSF identification simulation: (a) object. (b) estimated depths vs. truth (mean value and error bars).

3.2. Tests on real images

3.2.1. Motion blur

The first example shown in Fig. 4(a) is an image from [2]. The PSFs are 1D rectangular functions of length ranging from 1 to 8 pixels. The result of our method is shown in Fig. 4(b) with 1D patches of size 1×61 pixels and 30 % overlap. The result is obtained in 4 min in a Matlab implementation given an image size of 900×600 pixels. The jogger is clearly identified in the image and his mean motion corresponds to a PSF of 4 pixels which is the PSF announced in [2].

Our approach allows us to handle the case of various moving objects in the same image. Fig. 4(c) shows an image 225×210 with two moving objects: the vertical object on the lower part is moving horizontally while the other one moves vertically at a lower velocity. We consider a set of 19 binary 2D PSFs of size varying from 1×1 to 10×10 pixels, with only one row or one column non zero. Fig. 4(d) shows our PSF identification results for the image (c) obtained in 1 min. The patch size is 25×25 pixels. The green color corresponds to horizontal movements (PSF label from 2 to 10) and the blue color to vertical movements (PSF label from 11 to 19). In our

result we clearly distinguish the two objects with the correct direction of movement. Besides, the object in the upper part is correctly classified as slower than the other.

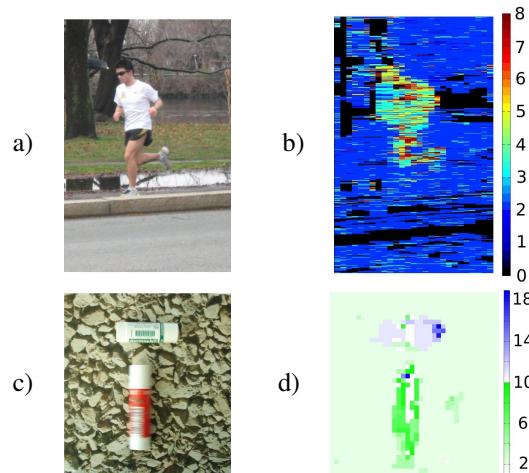


Fig. 4. (a) and (c) Real images: (a) is drawn from [2]. (b) and (d) are GL results. Label 0 denotes PSF not estimated.

3.2.2. Defocus blur

In this section we test our method on defocus blur identification. Fig. 5 shows results with the PSFs set and images of size 1170×1760 provided in [1] where a coded aperture is added to a camera. Fig. 5(b) shows the depth maps produced by our method. The colorbar gives the depth corresponding to the color label in cm. The patch size is 25×25 pixels with 50 % overlap. On textured patches our results are similar to the raw depth maps shown in [1, Figure 8.(b)]. Note that we have chosen to reject textureless regions, while [1] provides interpolated labels, thanks to a non convex deconvolution. However their computation time is much higher (few hours compared to 3 min for our method) and our result could be smoothed a posteriori using graphcuts techniques as in [1, 7].

4. CONCLUSION

We have proposed to address the identification of spatially varying blur using a single image by the means of a local likelihood to be maximized with respect to a PSF label and a SNR parameter. The PSF label is related to a set of candidate PSFs which has to be defined beforehand by calibration or modeling. The main technical contribution is an efficient algorithm for likelihood computation and maximization without resorting to inadequate periodic boundary conditions. The resulting identification method is fast and has demonstrated good performance on simulated and real examples originating from motion blur identification and depth from defocus. The proposed criterion could be used directly in a regularisation framework for depth or motion segmentation.

5. ACKNOWLEDGEMENT

This work was sponsored by the Direction Générale de l'Armement (DGA) of the French Ministry of Defense.

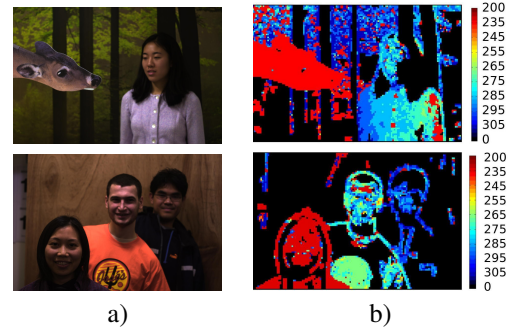


Fig. 5. a) Real images taken from [1]. b) Depth maps obtained with our method (label 0 denotes PSF not estimated).

6. REFERENCES

- [1] A. Levin, R. Fergus, F. Durand, and W.T. Freeman, "Image and depth from a conventional camera with a coded aperture," *ACM Trans. Graph.*, vol. 26, no. 3, pp. 1–9, 2007.
- [2] A. Chakrabarti, T. Zickler, and W.T. Freeman, "Analyzing spatially-varying blur," in *Proc. Conf. Computer Vision and Pattern Recognition*. IEEE, 2010, pp. 2512–2519.
- [3] R. Fergus, B. Singh, A. Hertzmann, S.T. Roweis, and W.T. Freeman, "Removing camera shake from a single photograph," *ACM Trans. Graph.*, vol. 25, no. 3, pp. 787–794, 2006.
- [4] A. Levin, Y. Weiss, F. Durand, and W.T. Freeman, "Understanding and evaluating blind deconvolution algorithms," in *Proc. Conf. Computer Vision and Pattern Recognition*. IEEE, 2009, pp. 1964–1971.
- [5] D. Kundur and D. Hatzinakos, "Blind image deconvolution," *Signal Processing Mag., IEEE*, vol. 13, no. 3, pp. 43–64, 1996.
- [6] Y.W. Tai and M. S. Brown, "Single image defocus map estimation using local contrast prior," *Image Processing (ICIP)*, pp. 1797–1800, 2009.
- [7] S. Zhuo and T. Sim, "On the recovery of depth from a single defocused image," in *Computer Analysis of Images and Patterns*. Springer, 2009, pp. 889–897.
- [8] N. Joshi, R. Szeliski, and D.J. Kriegman, "PSF estimation using sharp edge prediction," in *Proc. Conf. Computer Vision and Pattern Recognition*. IEEE, 2008, pp. 1–8.
- [9] M. Martinello, T.E. Bishop, and P. Favaro, "A Bayesian approach to shape from coded aperture," in *Image Processing (ICIP)*. IEEE, 2010, pp. 3521–3524.
- [10] AN Rajagopalan and S. Chaudhuri, "Performance analysis of maximum likelihood estimator for recovery of depth from defocused images and optimal selection of camera parameters," *International Journal of Computer Vision*, vol. 30, no. 3, pp. 175–190, 1998.
- [11] J. Idier, Ed., *Bayesian approach to inverse problems*. ISTE Ltd and John Wiley & Sons Inc, apr. 2008.
- [12] A. Neumaier, "Solving ill-conditioned and singular linear systems: A tutorial on regularization," *Siam Review*, vol. 40, no. 3, pp. 636–666, 1998.